Asian Journal of Physical and Chemical Sciences

Volume 12, Issue 3, Page 41-56, 2024; Article no.AJOPACS.125629
ISSN: 2456-7779

Determination the Anticorrosive Properties of Trimebutine Maleate for Aluminum Corrosion in 2M HCl Gravimetric and Quantum Chemistry Approaches

M. Cissé [a*], L.A.C. Koffi [a], M. Yéo [b], K.R. Kouamé [a], M. A. Tigori [a], Y. Bakouan [c] and P. M. Niamien [b]

[a] Laboratoire des Sciences et Technologies de l'Environnement, UFR Environnement, Université Jean Lorougnon Guédé, BP 150 Daloa, Côte d'Ivoire.
[b] Laboratoire de Constitution et de Réaction de la Matière, UFR SSMT, Université Félix Houphouët-Boigny, Abidjan, Côte d'Ivoire.
[c] Laboratoire de Chimie Moléculaire et des Matériaux (LC2M), UFR SEA,Université Joseph KI-ZERBO, 03 BP 7021 Ouagadougou 03, Burkina Faso.

Authors' contributions

This work was carried out in collaboration among all authors. All authors read and approved the final manuscript.

Article Information

DOI: https://doi.org/10.9734/ajopacs/2024/v12i3230

Open Peer Review History:
This journal follows the Advanced Open Peer Review policy. Identity of the Reviewers, Editor(s) and additional Reviewers, peer review comments, different versions of the manuscript, comments of the editors, etc are available here: https://www.sdiarticle5.com/review-history/125629

Original Research Article

Received: 24/08/2024
Accepted: 27/10/2024
Published: 04/11/2024

**Corresponding author: E-mail: mbouille.cisse07@gmail.com;*

Cite as: *Cissé, M., L.A.C. Koffi, M. Yéo, K.R. Kouamé, M. A. Tigori, Y. Bakouan, and P. M. Niamien. 2024. "Determination the Anticorrosive Properties of Trimebutine Maleate for Aluminum Corrosion in 2M HCl Gravimetric and Quantum Chemistry Approaches". Asian Journal of Physical and Chemical Sciences 12 (3):41-56. https://doi.org/10.9734/ajopacs/2024/v12i3230.*

ABSTRACT

The present work evaluated the inhibition properties of (R,S)-2-(dimethylamino)-2-phenylbutyl 3,4,5-trimethoxybenzoate or trimebutine maleate (TM) in aluminum corrosion in 2M hydrochloric acid. Tests were carried out using gravimetric methods and density functional theory (DFT). The results indicate that trimebutine maleate is a good inhibitor of aluminum corrosion in 2M hydrochloric acid at low temperatures. Indeed, the inhibition efficiency of this molecule increases with increasing concentration and decreases with increasing temperature. For an inhibitor concentration of 5.2mM and at 298K, we obtained an inhibition efficiency of 93.61%. The adsorption process is spontaneous, exothermic and follows the Langmuir model. The activation parameters were calculated and analyzed. DFT at the B3LYP/6-311G (d.p) level was used to determine molecular parameters such as E_{HOMO}, E_{LUMO}, ΔE, η, S, μ , A, I, χ, ΔN, ω. These theoretical parameters showed that TM is highly reactive and can both donate and receive electrons from aluminum. They thus confirmed the good inhibition performance of the molecule studied. These parameters were used to explain the inhibition efficiencies obtained. Local selectivity was analyzed using Fukui functions and the dual descriptor to determine possible nucleophilic and electrophilic attack sites.

Keywords: Trimebutine maleate; corrosion; aluminum; hydrochloric acid; density functional theory; gravimetric methods.

1. INTRODUCTION

The search for corrosion inhibitors capable of reducing metal corrosion has become a major preoccupation for researchers in this field [1]. Corrosion causes enormous material damage, which continues to have a negative impact on the economies of many industrial sectors [2].
However, corrosion can be controlled by numerous methods, including corrosion inhibitors. In this context, several organic compounds have been used to prevent aluminum corrosion in hydrochloric acid solutions [3,4,5,6].

Aluminum and its alloys due to their low cost, light weight, low density, good appearance and high thermal and electrical conductivity are widely used in many businesses [7]. In use, aluminum and its alloys become coated with corrosion products. Hydrochloric acid, for example, is used to maintain aluminum equipment [8].

Research has been carried out to find inexpensive, non-toxic, natural and eco-friendly inhibitors for the protection of metals and alloys against corrosion in acid solutions during this maintenance [9,10,11]. Some organic and inorganic corrosion inhibitors effective in combating metal degradation in said acid solutions are toxic [12]. Their use poses problems for the environment and human health. In recent studies, researchers have turned to green sources or plant extracts and drugs [13,14,15]. These efforts directed towards these compounds are justified by their accessibility and non-toxicity. Compounds containing heteroatoms or heterocycles have the ability to slow down the dissolution of aluminum in acid solutions and replace toxic inhibitors.

These compounds or molecules, by virtue of their structure containing atoms (O, N and S), are likely to bind to the aluminum surface to form an adsorption layer. This type of layer reduces the loss of electrons from the metal in the aggressive solution. Based on this information, drugs such as antivirals [16], antihypertensives [17], antihistamines [18], antidiabetics [19] and vitamins [20] have been used to inhibit metal corrosion. Therefore, this study consists in testing the inhibition properties of (R,S)-2-(dimethylamino)-2-phenylbutyl 3,4,5-trimethoxybenzoate or trimebutine maleate in aluminum corrosion in 2M HCl. This compound is an antispasmodic, as it is used in the symptomatic treatment of spasmodic intestinal pain. It helps relieve transit disorders and intestinal discomfort associated with functional bowel problems.

In this study, DFT, a theoretical method, was used to accompany the experimental method. This combination will help explain the inhibition mechanism as well as the electronic exchanges between the molecule and the metal. Specifically, inhibitory efficiencies, adsorption type, adsorption and activation thermodynamic quantities, and local and global reactivity quantum descriptor parameters were determined.

2. MATERIALS AND METHODS

2.1 Solution Test Preparation

All reagents and solvents used in the experiment were of analytical grade and used without further purification. The aggressive solution of 2.0 M HCl was prepared by diluting the analytical grade 37% (Merck Chemicals) with distilled water. Acetone from Sigma Aldrich with purity: 99.5%. The inhibitor trimebutine maleate (Fig. 1) was acquired from Sinopharm chemical reagent. Four concentrations have been prepared from this inhibitor which are 0.26mM; 0.52mM; 1.3mM; 5.2mM.

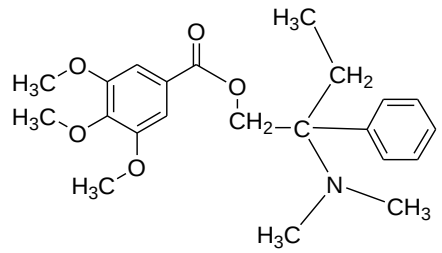

Fig. 1. Chemical structure of trimebutine maleate (TM)

2.2 Aluminum Samples Preparation

The aluminum samples were in the form of rod measuring 10mm in length and 2mm in diameter. The samples were polished with abrasive paper ranging from 150 to 600 grit, cleaned with acetone, washed with distilled water and dried in an oven. The samples were then weighed (m_1).

2.3 Weight Loss Measurements

Each sample is immersed in 50 mL HCl-2M with or without the various concentrations of trimebutine maleate. After 1h immersion, the sample is removed from the solution and rinsed thoroughly with distilled water. It is dried, then reweighed (m_2). Each test was repeated at 298 K, 308 K, 318 K, 328 K and 338 K.
Weight loss measurements ($\Delta m = m_1 - m_2$) were used to deduce the average corrosion rate of aluminum (W), the rate of surface coverage (θ) and the inhibitor inhibition efficiency IE(%) as a function of set temperature and inhibitor concentration. These parameters were obtained from the following equations:

- $W = \frac{m_1 - m_2}{S_e.t}$ (1)
- $\theta = \frac{W_0 - W}{W_0}$ (2)
- $IE(\%) = \frac{W_0 - W}{W_0} * 100$ (3)

Where: S_e is the surface of aluminum, t is the immersion time.
W_0 and W; are respectively aluminum corrosion rate in absence and presence of TM

2.4 Thermodynamic Adsorption and Activation Determination Method

The possibility of the adsorption reaction is indicated by the variation in standard free enthalpy of adsorption ΔG^0_{ads}. This quantity is determined from the relationship below [21].

- $\Delta G^0_{ads} = RTln\,(55.5\,K_{ads})$ (4)

Where : K_{ads} is the adsorption constant, 55.5 is the concentration of water (in mol/L) in the solution; R is the perfect gas constant; T is absolute temperature.

Quantities such as adsorption enthalpy (ΔH^0_{ads}) and adsorption entropy (ΔS^0_{ads}) are deduced from the Gibbs relation:

- $\Delta G^0_{ads} = \Delta H^0_{ads} - T\Delta S^0_{ads}$ (5)

Activation parameters such as activation energy (E_a), enthalpy activation (ΔH^*_a) and entropy activation (ΔS^*_a) are calculated from the following expressions

- $W = Aexp\left(-\frac{E_a}{RT}\right)$ (6)
- $W = \frac{R.T}{N_A.h} exp\left(\frac{\Delta S^*_a}{R}\right).exp\left(-\frac{\Delta H^*_a}{R.T}\right)$ (7)
- $log\left(\frac{W}{T}\right) = log\left(\frac{R}{N_A.h}\right) + \frac{\Delta S^0_a}{2,3.R} - \frac{\Delta H^0_a}{2,3.R.T}$ (8)

Where E_a is the activation energy, R is the perfect gas constant, T is the absolute temperature and A is the frequency factor. N_A is Avogadro's number.

2.5 Theoretical Approach: Quantum Chemical Calculations

DFT based on quantum chemical calculations was used to explain the experimental data.

Experimental results can be used to determine the inhibition efficiency of the molecule studied. While DFT can be used to explain the mechanism by which the molecule protects the metal. All calculations were performed with Gaussian 09 software using 6-311G (d, p) basis set [22] with Becke's three-parameter hybrid (B3LYP) [23]. Geometric optimization was carried out under the same conditions, and the relevant parameters were calculated. These parameters are highest occupied molecular orbital energy (E_{HOMO}), lowest unoccupied molecular orbital energy (E_{LUMO}),dipole moment (μ) and total energy (E_T). Using the mathematical relationships expressed below, other parameters such as energy gap (ΔE), ionization energy (*I*), electron affinity (*A*), electronegativity (χ), , softness (σ), hardness (η) and electrophylicity index (ω), fraction of electrons transferred (ΔN) have been determined [24,25,26,27,28, 29,30].

- $\Delta E = E_{LUMO} - E_{HOMO}$ (9)
- $I = -E_{HOMO}$ (10)
- $A = -E_{LUMO}$ (11)
- $\chi = \frac{I+A}{2} = -\frac{E_{LUMO}+E_{HOMO}}{2}$ (12)
- $\sigma = \frac{1}{\eta} = \frac{2}{I-A}$ (13)
- $\eta = \frac{I-A}{2} = \frac{E_{LUMO}-E_{HOMO}}{2}$ (14)
- $\omega = \frac{\mu_P^2}{2\eta} = \frac{(I+A)^2}{4(I-A)}$ (15)
- $\Delta N = \frac{\phi_{Al}-\chi_{inh}}{2(\eta_{Al}+\eta_{inh})}$ (16)

Where χ_{inh} and ϕ_{Al} represent electronegativities of the inhibiting molecule and the metal respectively while η_{inh} and η_{Al} represent the hardness of the inhibiting molecule and metal respectively. The theoretical value of Al ($\phi_{Al} = 4{,}28\ eV, and\ \eta_{Al} = 0$) were used to calculate the number of transferred electrons.

3. RESULTS AND DISCUSSION

3.1 Temperature and Inhibitor Concentration Action on Aluminum Corrosion Rate

Fig. 2 shows the evolution of corrosion rate as a function of TM concentration and reaction medium temperature.

Fig. 2 shows that the corrosion rate decreases progressively with increasing TM concentration. It also appears increasing temperature leads to a rapid change in the corrosion rate of aluminum. This rate increases sharply in the absence of inhibitor. These results clearly indicate that the addition of TM to the corrosive solution slows down aluminum dissolution. Hydrogen ions in solution promote aluminum oxidation. This oxidation, which increases with temperature, is reduced by the presence of trimebutine.

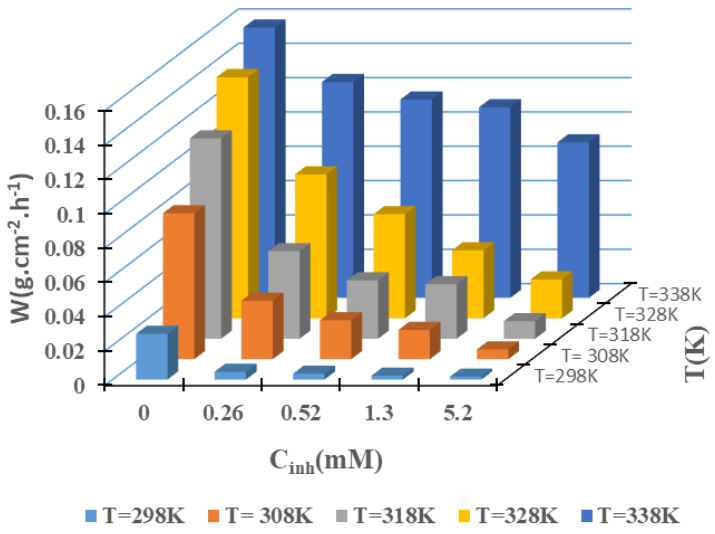

Fig. 2. Corrosion rate versus temperature and TM concentration

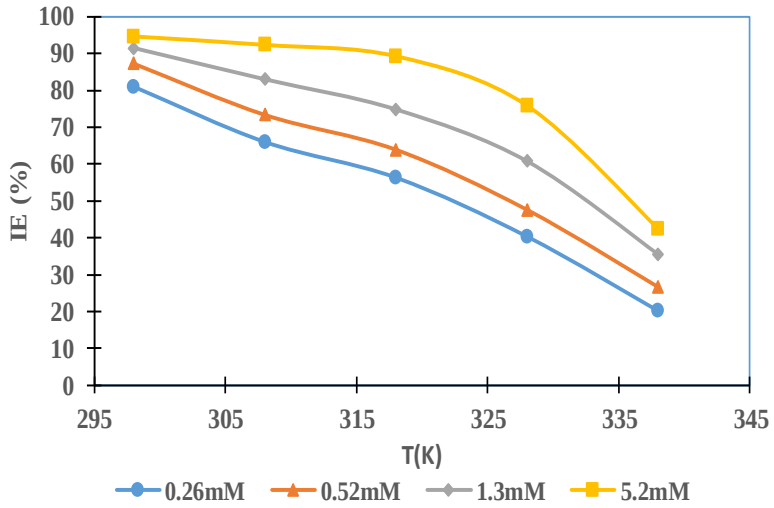

Fig. 3. Evolution of Inhibition Efficiency as a Function of Temperature

3.2 Influence of Temperature and Inhibitor Concentration on Inhibition Efficiency

The progression of inhibition efficiency as a function of TM concentration and reaction medium temperature is illustrated by Fig. 3.

Examination of Fig. 3 shows that the inhibition efficiency decreases as the temperature of the corrosive solution rises, and increases as the concentration of TM increases. These results show that the molecule adsorbs weakly to the aluminum surface as the temperature rises. In fact, the dissolution of aluminum in 1M HCl solution increases as temperature rises. Thus, when this loss of electrons becomes significant, the electrons supplied by trimebutine maleate are not sufficient to replace them, which explains why the efficiency of inhibition decreases with increasing temperature. The increase in inhibition efficiency with increasing concentration is due to the adsorption of trimebutine maleate on the aluminum surface. In addition, the adsorbed layer on the metal surface becomes increasingly compact as the inhibitor concentration increases. This adsorption is aided by the presence of oxygen and nitrogen atoms, electron pairs and π-electrons on the molecule's aromatic nuclei. The metal surface is thus covered with a protective layer that reduces the effects of oxidizing ions.

3.3 Adsorption Isotherm Studies

The study of the adsorption mode provides information on the characteristics of the TM adsorption process on the aluminum surface. The models of Langmiur, Temkin, El-Awady and Freundlich were tested in order to identify the one that correctly describes the behavior of TM on the metal surface. This study is based on the relationship between recovery rate (θ) and inhibitor concentration (C_{inh}). To determine the nature of adsorption, the Adejo-Ekwenchi model was used. The equations for these isotherms are given by the following relationships [31,32, 33,34,35]:

- Isotherme de Langmuir : $\frac{\theta}{1-\theta} = K_{ads}.C_{inh}$ (17)
- Isotherme de Temkin :

$$\theta = \frac{2{,}303}{f}[logK_{ads} + logC_{inh}] \quad (18)$$

- El-Awady :

$$log\left(\frac{\theta}{1-\theta}\right) = \log K_{ads} + ylogC_{inh} \quad (19)$$

- Freundlich: $\theta = K_{ads}\,.\,C_{inh}{}^{1/n}$ (20)
- Adejo- Ekwenchi :
- $log\left(\frac{1}{1-\theta}\right) = logK_{AE} + blogC_{inh}$ (21)

Where, f : coefficient related to lateral interactions between molecules in the adsorption layer, K_{ads}: adsorption equilibrium constant, $1/y = x$ expresses the number of active sites occupied by an inhibitor molecule; b is the

parameter of the Adejo Ekwenchi isotherm and K_{AE}: adsorption equilibrium constant of the Adejo Ekwenchi model.

Figs. 4, 5, 6 and 7 illustrate the representations of the different isotherms. The parameters of the isotherms studied are given in Table 1.

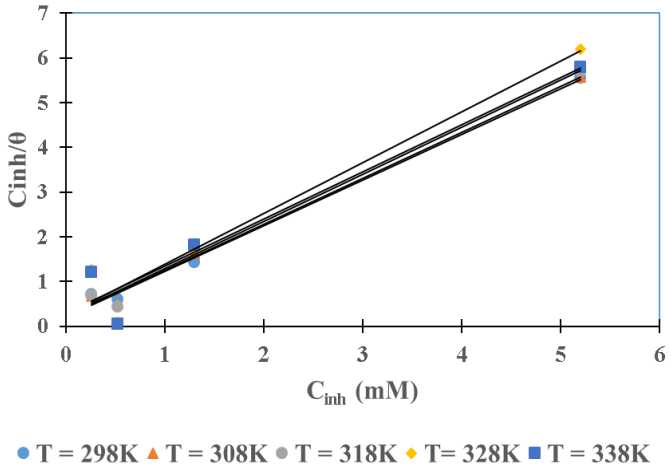

Fig. 4. Langmuir adsorption isotherm plots of TM on aluminum in 2M HCl

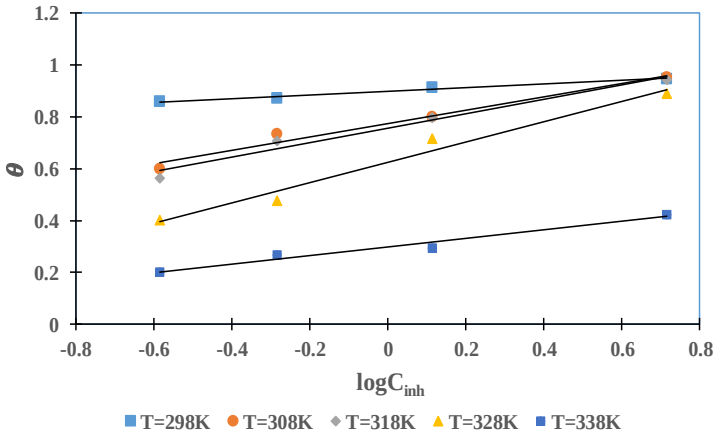

Fig. 5. Langmuir adsorption isotherm plots of TM on aluminum in 2M HCl

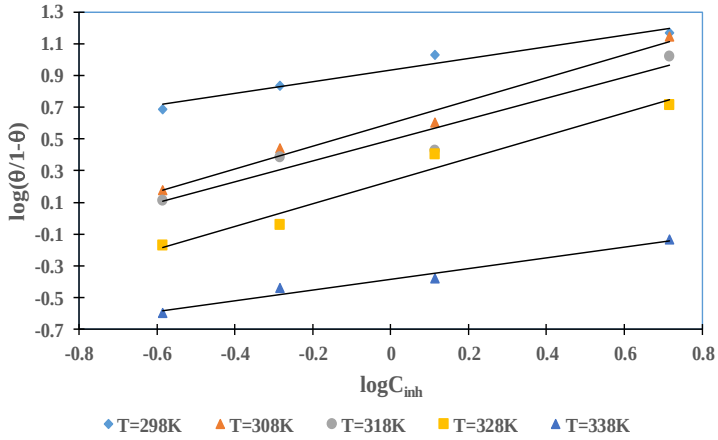

Fig. 6. EL-Awady adsorption isotherm plots of TM on aluminum in 2M HCl

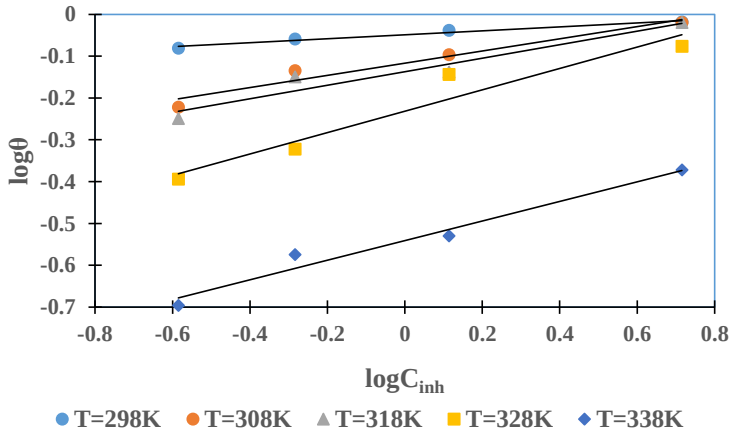

Fig. 7. Freundlich adsorption isotherm plots of trimebutine on aluminum in 2M HCl

Table 1. Isotherms parameters for various temperatures

Isotherms	T(K)	Slope	Intercept	(R^2)
	298	1.0208	0.2133	0.9944
	308	1.0291	0.2208	0.9942
Langmuir	318	1.0541	0.2357	0.9958
	328	1.0417	0.2464	0.9934
	338	1.0542	0.2968	0.9955
	298	0.0697	0.899	0.9745
	308	0.2580	0.7742	0.9747
Temkin	318	0.2790	0.7559	0.9713
	328	0.3917	0.6252	0.9720
	338	0.1642	0.2984	0.9707
	298	0.3685	0.9337	0.9625
	308	0.722	0.5980	0.9816
El-Awady	318	0.6572	0.4922	0.9338
	328	0.7164	0.2342	0.9711
	338	0.3397	0.3840	0.9732
	298	0.0470	-0.0489	0.9695
	308	0.1456	-0.1169	0.9522
Freundlich	318	0.1615	-0.1375	0.9320
	328	0.2553	-0.2319	0.9293
	338	0.2344	-0.5410	0.9694

Analysis of the parameters of the lines for the various isotherms indicates that the coefficients of determination (R^2) for the Langmuir model are closer to unity than those for the other models. In addition, the slopes of the Langmuir isotherm lines are approximately equal to one. Consequently, the adsorption of TM follows Langmuir adsorption model. During adsorption of the inhibitor on aluminum surface, each site can adsorb only one particle and the adsorption energy is constant. Furthermore, interactions between adsorbed particles are negligible [30].

The Adejo-Ekwenchi isotherm has been used to specify the nature of adsorption, i.e. the temperature ranges where chemisorption and physisorption take place [35]. The representation of this isotherm is given in Fig. 8. The parameters of this isotherm are given in Table 2.

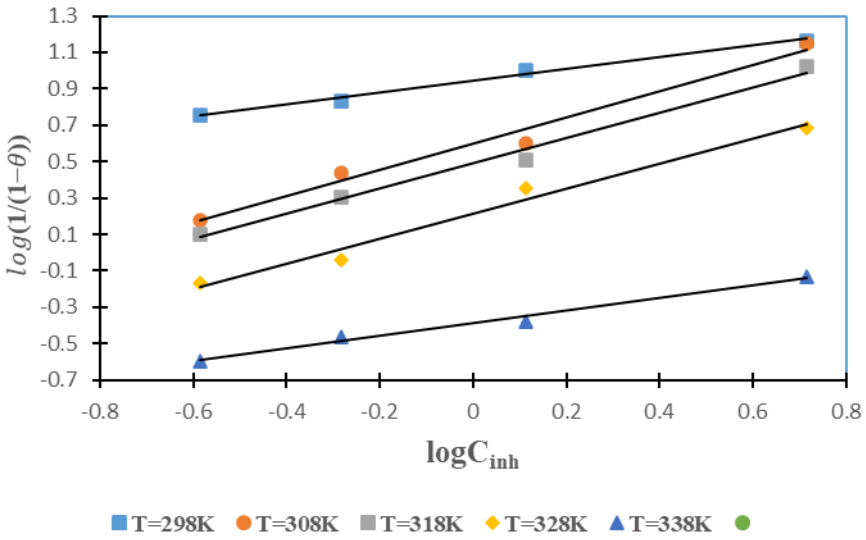

Fig.8. Adejo-Ekwenchi isotherm plots of trimebutine on aluminum in 2M HCl

variation of $log\left(\frac{1}{1-\theta}\right)$ as a function of $logC_{inh}$

Table 2. Values of thermodynamic adsorption quantities

T(K)	Equations	R^2
298	$log\left(\frac{1}{1-\theta}\right) = 0.3222logC_{inh} + 0.9432$	0.9917
308	$log\left(\frac{1}{1-\theta}\right) = 0.722logC_{inh} + 0.598$	0.9816
318	$log\left(\frac{1}{1-\theta}\right) = 0.6968logC_{inh} + 0.4901$	0.9888
328	$log\left(\frac{1}{1-\theta}\right) = 0.6859logC_{inh} + 0.2136$	0.9814
338	$log\left(\frac{1}{1-\theta}\right) = 0.3455logC_{inh} + 0.3889$	0.9854

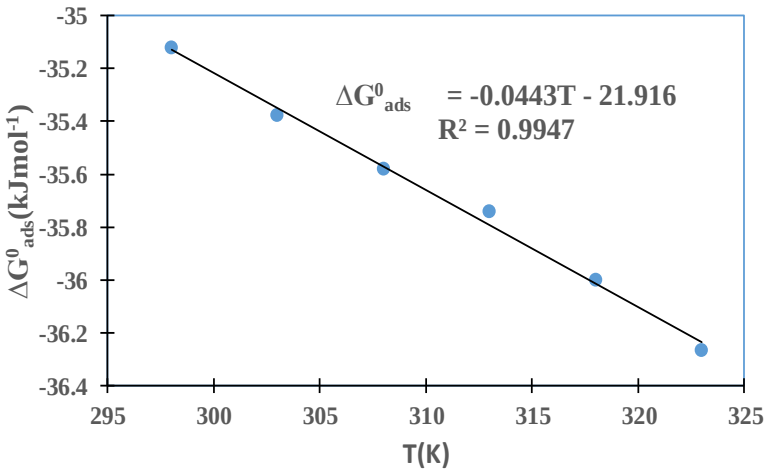

Fig. 9. Evolution of ΔG^0_{ads} as a function of temperature

Table 3. Values of thermodynamic adsorption quantities

T(K)	K_{ads}	ΔG^0_{ads} $(kJ.mol^{-1})$	ΔH^0_{ads} $(kJ.mol^{-1})$	ΔS^0_{ads} $(J.mol^{-1}K^{-1})$
298	4688.232536	-30.91562072		
308	4531.037608	-31.82736227		
318	4255.319149	-32.69481385	-21.916	44.300
328	4058.441558	-33.59383523		
338	3369.272237	-34.09531716		

The slopes of the straight lines obtained, which represent the parameter b of this isotherm, increase from 298K to 308K.This increase indicates that trimebutine maleate adsorbs to the metal by covalent bonds (chemical adsorption). On the other hand, the values of b decrease from 308K to 338K. In this case the molecule adsorbs to the aluminum surface by electrostatic interactions (physical adsorption). It can be deduced from this that the adsorption of the inhibitor on the aluminum surface is dominated by physisorption. This type of adsorption does not promote effective protection of the metal against corrosion at high temperatures [36].

3.4 Thermodynamic Study of the Inhibition Process

3.4.1 Thermodynamic quantities of adsorption

The changes in standard adsorption-free enthalpy values obtained from expression (3). These values were used to deduce the standard adsorption enthalpy (ΔH^0_{ads}) and entropy (ΔS^0_{ads}) change using Fig. 9. The values of these quantities are listed in Table 3.

The values of K_{ads} decrease progressively as the temperature increases. This decrease relates to the desorption of inhibitor molecules from the aluminum surface [31]. These molecules become increasingly detached from the aluminum surface as the temperature rises. These data explain the decrease in TM inhibition efficiency as the temperature rises. In this case, the increase in temperature is unfavourable to the adsorption of TM on metal surface in hydrochloric acid solution.

The values of ΔG^0_{ads} are negative, so the inhibitor adsorption process is spontaneous and the adsorbed layer is stable. In addition, the values of ΔG^0_{ads} are between -20 kJ.mol^{-1} and -40 kJ.mol^{-1}. In this case, the adsorption process is both chemical and physical [37,38]. The exothermicity of the adsorption process is indicated by negative values of ΔH^0_{ads} [39]. The positive values of ΔS^0_{ads} mention that this process is accompanied by an increase in disorder [39]. This disorder is due to the detachment of water molecules from the metal surface.

3.4.2 Thermodynamic activation factors

Representations of $logW$ as a function of $1/T$ (Fig. 10) and $\log(W/T)$ as a function of $1/T$ (Fig. 11) for different inhibitor concentrations allow the activation energy (E_a), activation enthalpy (ΔH^*_a) and activation entropy (ΔS^*_a) to be calculated.

Analysis of Table 4 shows that activation energy values in the inhibited solutions are higher than those in the control. These data show that aluminum dissolution is rapid in the absence of TM and slow in its presence. This dissolution becomes slower and slower as the concentration of the inhibitor increases. The enthalpy of activation values are positive and increase with inhibitor concentration. These values show that aluminum dissolution in HCl-2M is endothermic and is reduced in the presence of the inhibitor [40]. Moreover, the activation entropy values indicate that this reduction is accompanied by a decrease in disorder. Similar results have been obtained in previous studies [41].

3.5 Theoretical Analysis of the Inhibition Mechanism

3.5.1 Analysis of global reactivity parameters

The optimised structure of the molecule studied by DFT in B3LYP/6-311G(d,p) is given in Fig. 12. The global reactivity parameters are listed in Table 5.

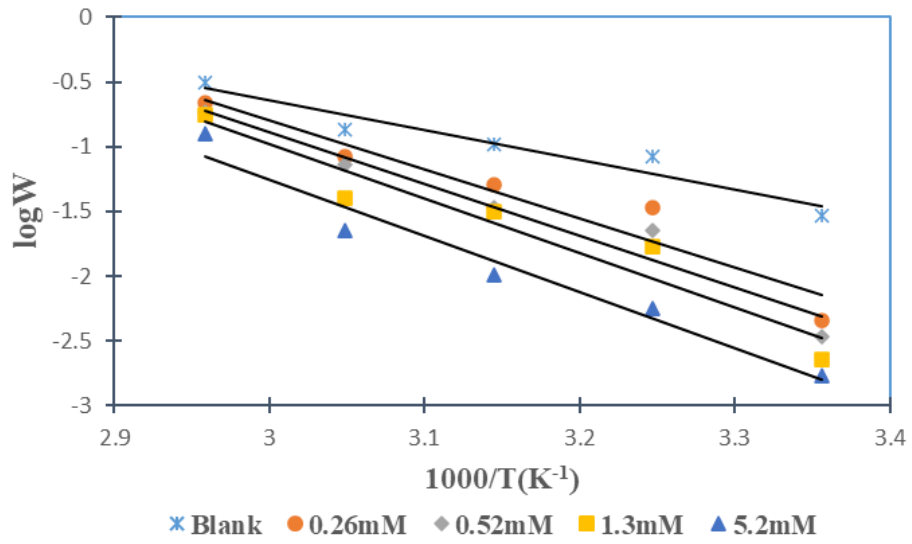

Fig. 10. Variation of $\log W$ **as function of** $1/T$

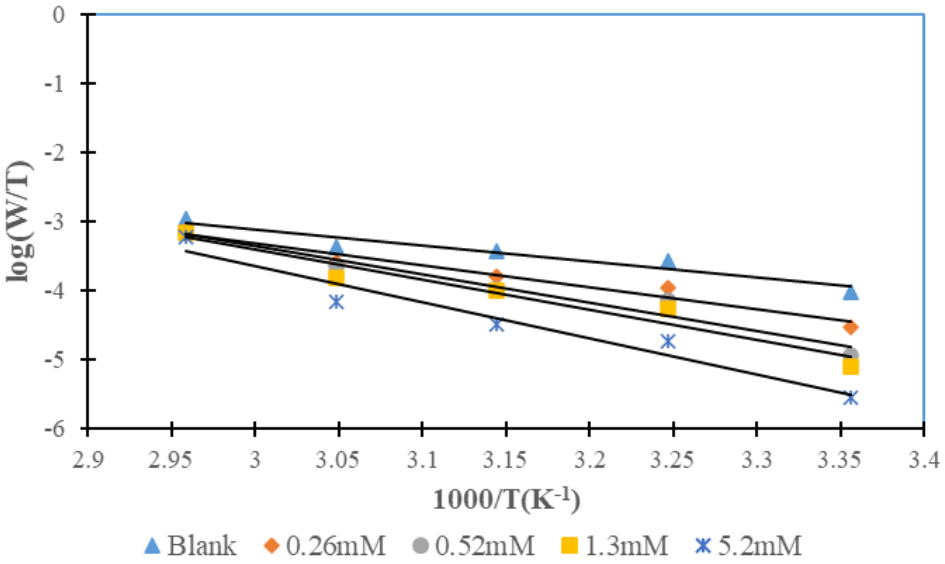

Fig. 11. Variation of $logW/T$ **as function of** $1/T$

Table 4. Thermodynamics Activation Parameters

C_{inh} (mM)	$E_a(kJ.mol^{-1})$	$\Delta H_a^*(kJ.mol^{-1})$	$\Delta H_a^*(kJ.mol^{-1})$
0	43.93991347	44.5511481	-123.5955968
0.26	73.03583123	60.70000518	-79.165632
0.26	77.09220646	78.19012947	-27.4525056
1.3	80.40705254	83.81578733	-11.5370944
5.2	83.31185408	100.0911068	32.646016

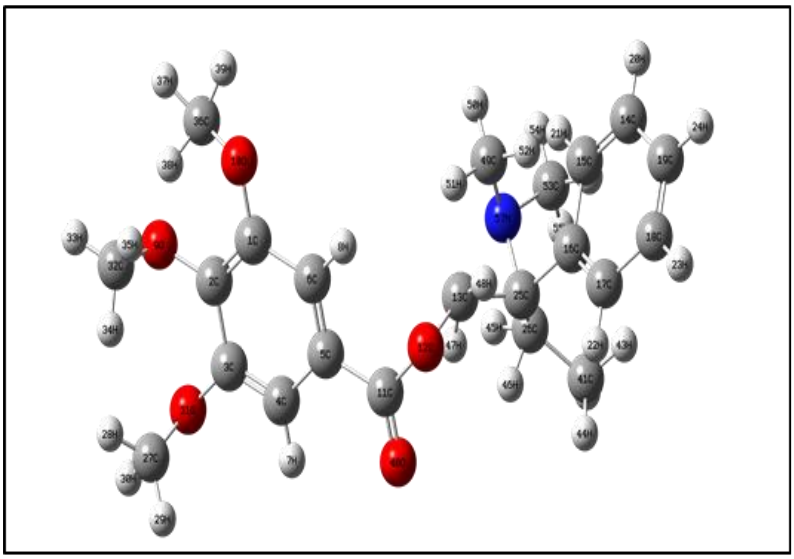

Fig. 12. Optimised structure of trimebutine maleate

Table 5. Global reactivity parameters of trimebutine maleat by B3LYP/6-31G(d, p)

Parameters	6-311G(d, p)
E_{HOMO} (eV)	-5.7952
E_{LUMO} (eV)	-2.5941
Energy gap ΔE (eV)	3.2011
Dipole moment μ (D)	5.2427
Ionization energy I (eV)	5.7952
Electron affinity A (eV)	2.5941
Electronegativity χ (eV)	4.1947
Hardness η (eV)	1.6006
Softness (σ) (eV)-1	0.6248
Fraction of electron transferred ΔN	0.0266
Electrophylicity index ω	5.4967
Energie totale E_T (Ha)	-1286.2922

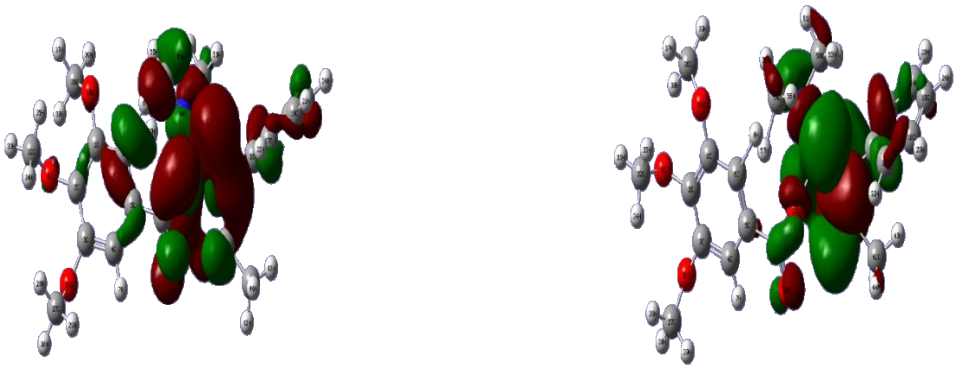

HOMO orbital **LUMO orbital**

Fig. 13. LUMO and HOMO molecular orbitals density distributions of trimebutine

Table 6. Mulliken atomic charges, Fukui functions and dual descriptor of trimebutine maleat by B3LYP/6-311G (d, p)

Atoms	$q_k(N+1)$	$q_k(N)$	$q_k(N-1)$	f_k^+	f_k^-	$\Delta f_k(\mathrm{r})$
1 C	0.006593	0.320657	-0.002456	-0.314064	0.323113	-0.637177
2 C	-0.004618	0.252848	0.128018	-0.257466	0.12483	-0.382296
3 C	0.002585	0.316542	-0.040039	-0.313957	0.356581	-0.670538
4 C	-0.00124	-0.135582	0.059392	0.134342	-0.194974	0.329316
5 C	0.000325	0.058641	0.00761	-0.058316	0.051031	-0.109347
6 C	0.002526	-0.13034	0.108356	0.132866	-0.238696	0.371562
7 H	0.000071	0.121994	-0.002936	-0.121923	0.12493	-0.246853
8 H	-0.000261	0.134077	-0.005251	-0.134338	0.139328	-0.273666
9 O	0.005721	-0.504444	-0.01697	0.510165	-0.487474	0.997639
10 O	0.035233	-0.54433	-0.012062	0.579563	-0.532268	1.111831
11 C	-0.001553	0.523937	0.183391	-0.52549	**0.340546**	**-0.866036**
12 O	0.008031	-0.521188	-0.00165	0.529219	-0.519538	1.048757
13 C	0.07198	0.069634	0.197821	0.002346	-0.128187	0.130533
14 C	0.086158	-0.178894	0.001872	0.265052	-0.180766	0.445818
15 C	0.062089	-0.116934	0.003863	0.179023	-0.120797	0.29982
16 C	0.037053	0.076503	-0.001414	-0.03945	0.077917	-0.117367
17 C	-0.025469	-0.151162	0.000827	0.125693	-0.151989	0.277682
18 C	0.086276	-0.112852	0.001309	0.199128	-0.114161	0.313289
19 C	-0.014494	-0.066134	-0.000177	0.05164	-0.065957	0.117597
20 H	-0.003562	0.073477	0.000012	-0.077039	0.073465	-0.150504
21 H	0.018948	0.103269	0.000199	-0.084321	0.10307	-0.187391
22 H	0.00067	0.089262	-0.000142	-0.088592	0.089404	-0.177996
23 H	-0.003151	0.077798	-0.00007	-0.080949	0.077868	-0.158817
24 H	0.001522	0.081005	0.000175	-0.079483	0.08083	-0.160313
25 C	-0.010496	-0.032399	-0.000309	0.021903	-0.03209	0.053993
26 C	0.003525	-0.232111	-0.001941	0.235636	-0.23017	0.465806
27 C	0.000117	-0.125157	-0.000403	0.125274	-0.124754	0.250028
28 H	-0.000039	0.12098	0.000393	-0.121019	0.120587	-0.241606
29 H	-0.000007	0.129352	0.000026	-0.129359	0.129326	-0.258685
30 H	-0.000002	0.137947	-0.000259	-0.137949	0.138206	-0.276155
31 O	-0.000034	-0.521641	0.000602	0.521607	-0.522243	1.04385
32 C	-0.000249	-0.095071	0.008689	0.094822	-0.10376	0.198582
33 H	-0.000026	0.133191	0.001989	-0.133217	0.131202	-0.264419
34 H	0.002857	0.109765	0.001441	-0.106908	0.108324	-0.215232
35 H	-0.000144	0.120314	-0.000791	-0.120458	0.121105	-0.241563
36 C	0.538722	-0.376941	0.174696	**0.915663**	-0.551637	**1.4673**
37 H	-0.037707	0.216559	-0.035661	-0.254266	0.25222	-0.506486
38 H	-0.011583	0.200869	0.065469	-0.212452	0.1354	-0.347852
39 H	-0.015435	0.190181	0.043525	-0.205616	0.146656	-0.352272
40 O	0.000572	-0.44954	0.074192	0.450112	-0.523732	0.973844
41 C	-0.000133	-0.320777	0.000308	0.320644	-0.321085	0.641729
42 H	0.000011	0.112275	-0.000003	-0.112264	0.112278	-0.224542
43 H	0.000245	0.113031	-0.00006	-0.112786	0.113091	-0.225877
44 H	-0.000003	0.116251	0.000034	-0.116254	0.116217	-0.232471
45 H	0.000661	0.14474	-0.000024	-0.144079	0.144764	-0.288843
46 H	0.001286	0.124103	0.008373	-0.122817	0.11573	-0.238547
47 H	-0.012284	0.124786	0.022245	-0.13707	0.102541	-0.239611
48 H	-0.005768	0.176185	0.004107	-0.181953	0.172078	-0.354031
49 C	-0.002307	-0.207423	0.002937	0.205116	-0.21036	0.415476
50 H	0.000976	0.095475	-0.000193	-0.094499	0.095668	-0.190167
51 H	0.001284	0.135413	-0.001399	-0.134129	0.136812	-0.270941
52 H	0.010493	0.164515	0.000008	-0.154022	0.164507	-0.318529
53 C	0.122651	-0.172226	0.013794	0.294877	-0.18602	0.480897

Atoms	$q_k(N+1)$	$q_k(N)$	$q_k(N-1)$	f_k^+	f_k^-	$\Delta f_k(\mathbf{r})$
54 H	-0.005648	0.150662	0.002915	-0.15631	0.147747	-0.304057
55 H	0.02092	0.129327	-0.000812	-0.108407	0.130139	-0.238546
56 H	0.011181	0.160569	-0.000172	-0.149388	0.160741	-0.310129
57 N	0.014929	-0.410989	0.006606	0.425918	-0.417595	0.843513

Molecular reactivity descriptors for TM have been calculated to explain the experimental values obtained. Indeed, the highest occupied molecular orbital energy (E_{HOMO}) obtained is high. Consequently, the molecule has the capacity to donate electrons to aluminum [42]. The lowest unoccupied molecular orbital energy (E_{LUMO}) obtained indicates that the molecule can receive electrons from the metal [42]. It has been reported that the adsorption of an inhibitor to a metal surface is often linked to its electron donor-acceptor relationship with the metal. The results indicate that the molecule studied can both donate and receive electrons from aluminum. These properties justify the high inhibition efficiencies obtained experimentally. In general, the energy gap (ΔE) of a corrosion inhibitor can be used to evaluate its reactivity. The higher the ΔE, the more stable the inhibitor molecule. The lower the ΔE, the more readily the inhibitor molecule is adsorbed onto the metal surface [43]. ΔE value obtained for trimebutine maleate is low. This molecule is therefore unstable and highly reactive. This reactivity confirms its strong adsorption to the metal surface.Moreover, the inhibition properties of a molecule depend on its values of overall hardness (η) and overall softness (σ) [43]. A molecule that has a high value of σ and a low value of η is likely to react with the metal to form covalent bonds. Whereas a molecule with a high η value and a low σ value is less reactive. The results indicate that trimebutine maleate has a low η value and a high σ value. This shows that TM is very reactive.

Ionisation energy (I) and electronic affinity (A), which are associated with HOMO and LUMO energies respectively, are descriptors of a molecule's reactivity [44]. These parameters describe the electronic exchanges between the molecule and the metal. The I and A values obtained show that trimebutine maleate has a strong capacity to supply electrons to aluminum.

The electronegativity value (χ) of trimebutine maleate (4.1947 eV) is lower than that of aluminum (4.28 eV), which justifies that the fraction of electrons transferred $\Delta N > 0$. Thus, there is a strong attraction of electrons towards aluminum [7]. This strong attraction that aluminum possesses will contribute to the replacement of its electrons lost during its oxidation in the corrosive medium HCl-2M. These data confirm the experimental values. The electrophilic character of the inhibitor is justified by its high value of the electrophilicity index (ω) [45]. The reaction activity of a molecule also depends on its total energy (E_T). In our work $E_T < 0$, this reflects that there is a charge transfer between the inhibitor and the aluminum [46].

The charge density distribution at each molecular orbital is shown in Fig. 13. This charge distribution describes the active regions of the inhibitor. Analysis of Fig. 13 indicates that the charge distribution at the HOMO and LUMO orbital is localised towards the nitrogen (N) atom, the carbon C(25) and π-bonds. The charge distribution around the nitrogen and C(25) indicates that these atoms are at the centre of the electronic exchanges allowing the formation of covalent bonds with the empty orbital of the metal. These data confirm the formation of the protective film as indicated by the gravimetric tests.

3.5.2 Analysis of local reactivity parameters

The local reactivity parameters were determined from the Fukui and dual descriptor functions. The values of these parameters are given in Table 6.

The values displayed in Table 6 reveal that C(11) atom has the lowest value of $\Delta f_k(r)$, while the C(36) atom has the highest value of f_k^+ and $\Delta f_k(r)$. In this context according to Martínez-Araya [47], C(11) and C(36) are respectively the likely sites for electrophilic and nucleophilic attacks. These sites are associated respectively with HOMO and LUMO orbitals of the molecule under study. These results explain the charge distribution around the C(36) atom

4. CONCLUSION

The use of corrosion inhibitors is a means of combating the dissolution of metals. The inhibition efficiency of aluminum corrosion in 2 M HCl by (R,S)-2-(dimethylamino)-2- phenylbutyl 3,4,5-trimethoxybenzoate or trimebutine maleate has been investigated using gravimetric measurement and quantum chemical

calculations at DFT/B3LYP/6-31G (d, p) level of theory. The following conclusions were drawn from this study:

- TM acts as a good inhibitor for corrosion of aluminum in 2.0 M HCl solution. The inhibition efficiency increases with increasing concentration.
- The inhibition action is performed via adsorption of the TM on aluminum surface. The adsorption process is spontaneous and follows Langmuir adsorption isotherm.
- Increasing temperature reduces TM inhibition efficiency, indicating that the adsorption process is dominated by physical adsorption.
- The presence of the extract increases the activation energy of the corrosion reaction.
- Quantum descriptors indicate that TM has a good capacity to accept and donate electrons to the metal.
- The sites of reactivity within the molecule were determined. These sites are mainly carbon atoms.

DISCLAIMER (ARTIFICIAL INTELLIGENCE)

Author(s) hereby declare that NO generative AI technologies such as Large Language Models (ChatGPT, COPILOT, etc.) and text-to-image generators have been used during the writing or editing of this manuscript.

COMPETING INTERESTS

Authors have declared that no competing interests exist.

REFERENCES

1. Jian Z et al. Combining experiment and theory researches to insight into anticorrosion nature of a novel thiazole derivative. Journal of the Taiwan Institute of Chemical Engineers, 2021;122: 190-200.
2. Ahmed YM, Abdul AHK, Abu BM, Mohd ST. Experimental and theoretical study on the inhibition performance of triazole compounds for mild steel corrosion. Corrosion Science. 2010; 52(10):3331-3340
3. Abdallah M et al. Appraisal of adsorption and inhibition effect of expired micardis drug on aluminum corrosion in hydrochloric acid solut. International Journal of Electrochemical Science, 2022;17(4): 220-462.
4. Nada A, Belal E, Ahmed F, Areej AlB, Arafat T. Investigation of expired ticarcillin and carbenicillin drugs for inhibition of aluminum corrosion in hydrochloric acid solution. International Journal of Electrochemical Science, 2022;17(12): 2212113.
5. Sumayah B, Abhinay T, Hassane LH, Ill-Min C, Kumar A. Corrosion inhibition efficiency of bronopol on aluminium in 0.5 M HCl solution: Insights from experimental and quantum chemical studies. Surfaces and Interfaces. 2020;20:100-542.
6. Khalid HR, Anees AK, Salman HA, Khalida FA-A, Hameed BM. Optimization studies of expired mouthwash drugs on the corrosion of aluminum 7475 in 1 M hydrochloric acid: Gravimetrical, electrochemical, morphological and theoretical investigations. Results in Surfaces and Interfaces. 2023;13:100-165.
7. Bashir Set al. Electrochemical behavior and computational analysis of phenylephrine for corrosion inhibition of aluminum in acidic medium. Metallurgical and Materials Transactions. 2019;50:468–479.
8. Eddy NO, Momoh-Yahaya H, Oguzie EE, Theoretical and experimental studies on the corrosion inhibition potentials of some purines for aluminium in 0.1 M HCl. Journal of Advanced Researc. 2015; 6(2):203-217.
9. Abdel Hameed RS, Ismail EA, Abu-Nawwas AH, Hussin IA-S, (Expired Voltaren Drugs as Corrosion Inhibitor for Aluminium in Hydrochloric Acid, International. Journal of Electrochemical Science. 2015;10(3):2098-2109.
10. Namrata C, Vinod KS, Quraishi MA, Papaya peel extract as potential corrosion inhibitor for Aluminium alloy in 1M HCl: Electrochemical and quantum chemical study, Ain Shams Engineering Journal. 2018; 9(4):1131-1140.
11. Tianqi C, Hui G, Zhan C, Mengjin C, Chaoyang Fu,Eco-friendly approach to corrosion inhibition of AA5083 aluminum alloy in HCl solution by the expired Vitamin B1 drugs. Journal of Molecular Structure. 2021;1244:130-881
12. Zhang W, Buchheit RG, Effect of ambient aging on inhibition of oxygen reduction by chromate conversion coatings. Corrosion. 2003;59(4):356-362.
13. Abdelkader K, Abdellah K, Kamel H, Razika M, Thymus algeriensis extract as a

new eco-friendly corrosion inhibitor for 2024 aluminium alloy in 1M HCl medium. Journal of Molecular Liquids. 2016;214(201):293-297.
14. Desai PS, Falguni D, Adarsh P, Bhumika P, Anticorrosive properties of Eucalyptus (Nilgiris) leaves extract on 2S grade aluminium in acid solutions. Applied Surface Science Advances. 2023;16:400-41.
15. Radouane et al. Experimental assessment and molecular-level exploration of the mechanism of action of Nettle (*Urtica dioica* L.) plant extract as an eco-friendly corrosion inhibitor for X38 mild steel in sulfuric acidic medium, Arabian Journal of Chemistry. 2023;16(8):104-988.
16. Ebenso EE, Arslan T, Kandemirli FNC, Love I, Quantum chemical studies of some rhodanine azosulpha drugs as corrosion inhibitors for mild steel in acidic medium. International Journal of Quantum Chemical. 2010;110:1003-1018.
17. Abdallah M, Zaafarany I, Al-Karanee SO, Abd El-Fattah AA. Antihypertensive drugs as an inhibitor for corrosion of aluminum and aluminum silicon alloys in aqueous solutions, Arabian Journal of Chemistry. 2012;5:225-234.
18. Amadou K, et al. Copper Corrosion Inhibition in 1M HNO3 by Loratadine: A Combined Experimental and Theoretical Study. International Journal of Materials and Chemistry. 2020 10(3): 31-43
19. Tigori MA, Kouyaté A, Assouma DAC, Kouakou V, Niamien PM, Theoretical Investigation of Two Antidiabetics Drugs as Corrosion Inhibitors of Aluminium in 1.0 M HCl: Combining DFT and QSPR Calculations. American Journal of Materials Science and Engineering. 2020;8(1):6-16
20. Yeo M, Tigori MA, Amadou KA, Niamien PM, Trokourey A, Inhibition of Aluminium Corrosion in 1M HCl by Pyridoxine Hydrochloride: Thermodynamic and Quantum Chemical Studies. International Research Journal of Pure & Applied Chemistry, 2020;15:19
21. Cissé M, Tigori MA, Assoman KA, Kouyaté A, Niamien PM, Gravimetric and quantum chemical approach of nifuroxazid as inhibitor of aluminium corrosion in 2.0 M HCl. Journal of Materials Physics and Chemistry. 2024;12(1):1-10.
22. Frisch M et al. Gaussian 09. Gaussian, Inc., Wallingford CT; 2009.
23. Lee C, Yang W, Parr RG, Development of the Colle-Salvetti correlation-energy formula into a functional of the electron density. Physical Review B. 1988;37:785.
24. Kumara D, Jain N, Rai B, Amino acids as copper corrosion inhibitors: A density functional theory approach. Applied Surface Science. 2020;514:145-905
25. Yang B, Yizhen L, Zhang Z, Xinying H, Zhu Y, Anticorrosion mechanism of natural acidic amino acids on steel in chloride solution: Experimental, theoretical and machine learning approaches. Journal of Building Engineering. 2023;79:107-801.
26. Parr RG, Pearson RG, Absolute hardness: companion parameter to absolute electronegativity. Journal of the American Chemical Society. 1983;105(26):7512-7516.
27. Chirico N, Gramatica P, Real external predictivity of QSAR models. Part 2. New intercomparable thresholds for different validation criteria and the need for scatter plot inspection. Journal of Chemical Information and Modeling, 2012;52(8) 2044-2058.
28. Pearson RG, Absolute electronegativity and hardness correlated with molecular orbital theory. Proceedings of the National Academy of Sciences. 1986; 83(22), 8440-8441.
29. Parr RG, Szentpály LV, Liu S, Electrophilicity index. Journal of the American Chemical Society. 1999;121(9), 1922-1924.
30. Cissé M, Tigori MA, Assoman KA, Kouyaté A, Niamien PM, Gravimetric and Quantum Chemical Approach of Nifuroxazid as Inhibitor of Aluminium Corrosion In 2.0 M HCl. Journal of Materials Physics and Chemistry. 2024;12(1):1-10.
31. Langmuir I, The constitution and fundamental properties of solids and liquids, Journal of the American Chemical Society. 1916; 38(11):2221–2295.
32. Temkin MI, Adsorption equilibrium and process Kinetics on inhomogeneous surfaces with interaction between adsorbed molecules. Zhurnal Fizicheskoi Khimii. 1941;15(3):296-332.
33. Freundlich H, Uber die adsorption in losungen, Zeitschrift fur Physikalische Chemie. 1906; 57:385–470.
34. Awady YAE, Ahmed AI, Effect of temperature and inhibitors on the corrosion of aluminium in 2N HCl solution,

A kinetic study. Journal of Indian Chemistry. 1985;24:601-606.
35. Adejo SO, Proposing a new empirical adsorption isotherm known as Adejo-Ekwenchi isotherm. Journal of Applied Chemistry. 2014;6(5);66-71.
36. Adejo SO, Ahile JU, Gbertyo JA, Kaior A, Ekwenchi MM, Resolution of adsorption characterisation ambiguity through the Adejo-Ekwenchi adsorption isotherm: A case study of leaf extract of Hyptis suaveolen poit as green corrosion inhibitor of corrosion of mild steel in 2 M HCl. Journal of Emerging Trends in Engineering and Applied Sciences. 2014;5(8):201-205.
37. Abdallah M et al. Natural nutmeg oil as a green corrosion inhibitor for carbon steel in 1.0 M HCl solution: Chemical, electrochemical, and computational methods. Journal of Molecular Liquids. 2021;323:115036.
38. Toghan A, Gadow HS, Dardeer HM, Elabbasy HM, New promising halo-genated cyclic imides derivatives as potential corrosion inhibitors for carbon steel in hydrochloric acid solution. Journal of Molecular Liquids. 2021;325:115-136.
39. Allah MD, El Hefnawy M, Elhamed SA, Experimental investigation of the corrosion inhibition of Aluminum by three novel anionic surfactants as green inhibitors in HCl solution. Chemical Data Collections. 2023;45:101033.
40. Singh AK, Mohapatra S, Pani B, Corrosion inhibition effect of Aloe Vera gel: Gravimetric and electrochemical study. Journal of Industrial and Engineering Chemistry. 2016;33:288-297.
41. Zeng J, Gan Y, Xu Z, Zhu H, Tan B, Li W, Adsorption films based on indazole derivatives for application to protect Cu in sulfuric acid: Experimental and theoretical approaches. Journal of the Taiwan Institute of Chemical Engineers. 2023;151: 105-134.
42. Issaadi S, Douadi T, Chafaa S, Adsorption and inhibitive properties of a new heterocyclic furan Schiff base on corrosion of copper in HCl 1M: Experimental and theoretical investigation.Applied Surface Science. 2014;316:582-589.
43. Ebaz AO, Karzan MA, Shalaw KS, Karzan AO, Wali MH, Dyari MM, N,N-Bis (2,4-dihydroxy benzaldehyde) benzidine: Synthesis, characterization, DFT, and theoretical corrosion study. Journal of Molecular Structure. 2024;1300: 137-279.
44. Zhang SG, Lei W, Xia MZ & Wang FY, QSAR Study on N-Containing Corrosion Inhibitors: Quantum chemical approach assisted by topological index. Journal of Molecular Structure: THEOCHEM. 2005; 732:173-182.
45. Ahmed A, Corrosion inhibition effect of 2-N-phenylamino-5-(3-phenyl-3-oxo-1-propyl)-1,3,4-oxadiazole on mild steel in 1 M hydrochloric acid medium: Insight from gravimetric and DFT investigations, Materials Science for Energy Technologies. 2021;4:398-406.
46. Tigori MA, Kouyaté A, Kouakou V, Niamien PM, Trokourey A, Computational approach for predicting the adsorption properties and inhibition of some antiretroviral drugs on copper corrosion in HNO_3. European Journal of Chemistry. 2020;11(3):235-244.
47. Martínez-Araya JI, Why is the dual descriptor a more accurate local reactivity descriptor than Fukui functions? The Journal of Mathematical Chemistry. 2015;53:451–465.

Peer-review history:
The peer review history for this paper can be accessed here:
https://www.sdiarticle5.com/review-history/125629